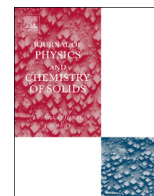




ELSEVIER

Contents lists available at ScienceDirect

Journal of Physics and Chemistry of Solids

journal homepage: www.elsevier.com/locate/jpcs

Electrochemical effects of isolated voids in uranium dioxide

A.-R. Hassan^a, Anter El-Azab^{a,*}, Michele Manuel^b^a School of Nuclear Engineering, Purdue University, West Lafayette, Indiana 47906, USA^b Department of Materials Science and Engineering, University of Florida, Gainesville, Florida 32611, USA

ARTICLE INFO

Article history:

Received 6 September 2013

Received in revised form

27 November 2013

Accepted 18 December 2013

Available online 27 December 2013

Keywords:

A. Oxides

D. Defects

D. Electrochemical properties

D. Microstructure

ABSTRACT

We present a model to study the electrochemical effects of voids in oxide materials under equilibrium conditions and apply this model to uranium dioxide. Based on thermodynamic arguments, we claim that voids in uranium dioxide must contain oxygen gas at a pressure that we determine via a Kelvin equation in terms of temperature, void radius and the oxygen pressure of the outside gas reservoir in equilibrium with the oxide. The oxygen gas within a void gives rise to ionosorption and the formation of a layer of surface-charge on the void surface, which, in turn, induces an influence zone of space charge into the matrix surrounding the void. Since the space charge is carried in part by atomic defects, it is concluded that, as a part of the thermodynamic equilibrium of oxides containing voids, the off-stoichiometry around the void is different from its remote bulk value. As such, in a uranium dioxide solid with a void ensemble, the average off-stoichiometry level in the material differs from that of the void-free counterpart. The model is applied to isolated voids in off-stoichiometric uranium dioxide for a wide range of temperature and disorder state of the oxide.

© 2013 Elsevier Ltd. All rights reserved.

1. Introduction

Extended defects are ubiquitous in all crystalline materials, including oxides, both under equilibrium and non-equilibrium conditions such as irradiation. Extended defects that have been widely studied in crystalline solids include interfaces and grain boundaries, dislocations lines and small dislocation loops, voids, bubbles and pores. Particle irradiation is effective in introducing extended defects such as loops, voids and bubbles [1]. Irradiation also leads, in some cases, to the formation of precipitates and it leads to evolution of the grain boundary network as in the case of grain growth and refinement in, say, nuclear fuel pellets [2]. Most of the extended defects induced by irradiation remain in the solid after the irradiation is stopped. The formation of extended defects under irradiation involves a process of nucleation and growth that is driven by the availability of point defects in excess of the thermal equilibrium concentrations. As a material of utmost technological importance in the nuclear industry, uranium dioxide, UO_2 , has been investigated for its formation of extended defects with and without irradiation over many decades [1,3]. Of special importance is the formation of voids or gas bubbles (cavities) in UO_{2+x} as this process affects both the mechanical properties, swelling, and thermal transport properties. Reactor-irradiated samples showed a dispersion of bubbles which would

coarsen and consolidate into larger equilibrium shaped cavities upon annealing as studied by TEM [3]. The position and size distribution of voids has been studied in the rim structure of the post-operation nuclear fuel elements [4]. More recently, mixed oxide fuel under short term irradiation was investigated by X-ray computer tomography and radiography and showed the formation of voids on the periphery of the fuel element [5]. Without irradiation, voids have also been found to form in UO_2 as part of the preparation of polycrystalline samples. Castell [6] used low voltage scanning electron microscopy for images of the equilibrium Wulff-shaped voids in UO_2 . The voids were produced by spectacular grain growth process that involved inclusion of intergranular pores into the grains. The finding showed the stability of coexisting voids in the oxide. The same phenomenon have also been found in other oxides depending on the preparation methods and were tied to changes in the physical properties of the oxides, see for example [7–9].

Efforts to simulate the formation of voids and dislocation loops have been carried out by means of Molecular Dynamics simulations. Martin et al. [10] used classical molecular dynamics simulations to investigate the clustering of irradiation-induced point defect into dislocation loops and nanocavities (voids). Defect clustering in ceria and urania has also been investigated by Aidhy et al. [11,12] by molecular dynamics. As to a higher scale, continuum mechanics models were introduced to tackle the interaction of voids in solids; such models analyzed the problem from a purely mechanical point of view serving the inquiry about mesoscale elements in metals and alloys. The work by Willis and

* Corresponding author. Tel.: +1 765 49 66864.

E-mail address: aelazab@purdue.edu (A. El-Azab).

Bullough [13], for example, attempted modeling of the mechanical interaction of two bubbles within a solid and predicted that they would always mechanically attract. Other attempts have also been proposed to model voids in solids through mechanical stress analysis [14]. However, such models were meant for metals and hence are not representative of other aspects of the problem that may arise in the case of oxides.

In order to properly model extended defects in an oxide such as UO_2 , the ionic nature of these materials must be taken into account. Charged point defects as well as electronic carriers are the building blocks of the oxides defective structures and the mediators of their evolution. The electrochemical and mechanical stress fields, both created by the defects, whether point or extended defects, dictate the stability or evolution of an oxide's defective elements. A set of investigations have been carried out in the past to take the ionic nature of oxides into consideration when modeling microstructure elements. The focus was mainly on dislocation loops [15–17]. Besides being limited to dislocation loops, such attempts have not considered the electronic structure modification in the form of intrinsic or extrinsic electronic states associated with extended defects, e.g., free surface, grain boundary, and so on; see [18,19]. To better model extended defects in oxides, we have introduced a local off-stoichiometry model that analyzed the interaction of defect fields in the presence of a flat surface exposed to equilibrium oxygen pressure [20]. The model was similar in spirit to the electrochemical and mechanical model of defects introduced by Swaminathan et al. [21], and, aside from being generalized to atomic defects and electronic charge carriers and gas reaction boundary conditions at the solid surface, it is formally equivalent to the classical space charge model of Kliewer and Koehler [22]. While there are many similarities in the electrochemical basis of this model to the ones introduced by Maier [23,24], this model, in addition to considering void effects, correlates the defect fields and the accompanying electrostatic profile to the chemical state of the oxide as controlled by the oxygen atmosphere. This effect comes into play on the bulk side by controlling the off-stoichiometry and on the surface side, in this case the void surface, as will be explained below. Here, we aim at the microstructure evolution of ionic UO_2 through interaction of mesoscale elements as mediated by defects and electronic carriers. Further, electronic structure results for the point defect formation energy and the electronic band structure was employed in application for the case of UO_{2+x} .

In light of the above, we bring into consideration the electrochemical effect of voids in oxides and their interaction with point defect fields. In this paper, we extend our model in [20] to the case of voids in UO_{2+x} . As shown in the next section, oxygen must be present inside the void as a result of chemical equilibrium of the overall material with a remote oxygen reservoir. The electrochemical effect arising due to the presence of oxygen inside voids is accounted for by the ionosorption theory. The defect fields around a void are then calculated within the framework of chemical diffusion of defects, which is based on the electro-chemical potentials of the defect and electronic species. In steady state, and in the absence of boundary fluxes, the defect concentration profiles are consistent with uniform electro-chemical potentials of all species. Such profiles represent the equilibrium profiles giving rise to the space charge profile and local off-stoichiometry of the oxide as a function of distance from the void surface.

2. Model

2.1. Oxygen pressure of isolated voids in an oxide

The uniform chemical state of a disordered oxide, such as UO_{2+x} , is controlled by the temperature and the oxygen pressure

of the chemical reservoir with which the oxide is in equilibrium. The presence of a void in the oxide perturbs this uniform state of equilibrium. In particular, as argued below, a void enclosed within a disordered oxide is required to adhere to thermodynamic equilibrium with the rest of the solid. This requires the void to contain oxygen gas, the pressure of which can be found by comparing the solid oxide with an isolated void with a reference void-free oxide subject to the same thermal and chemical environment.

The sought comparison can be made by considering a void remotely placed in a semi-infinite solid with a flat surface in contact with a reservoir of oxygen at partial pressure p_0 . Without loss of generality, the void is assumed to have a spherical shape with a radius R and oxygen content at pressure p . Thermodynamic equilibrium is assumed of the system. The oxygen chemical potential within the oxide equals that of the environment; that is

$$\mu_O^{\text{oxide}} = \frac{1}{2}\mu_{O_2}^0(T, p_0), \quad (1)$$

where μ_O^{oxide} is the potential within the solid oxide. Applying the same condition with the content of the void gives

$$\mu_O(T, p) = \mu_O^{\text{oxide}} = \frac{1}{2}\mu_{O_2}^0(T, p_0), \quad (2)$$

which gives the chemical equilibrium condition. On the other hand, mechanical equilibrium of the void surface requires

$$p - p' = \frac{2\gamma}{R}, \quad (3)$$

where p' is the mechanical pressure in the oxide just outside the void surface and γ is the oxide surface energy. Eqs. (2) and (3) furnish the necessary conditions for equilibrium [25]. A perturbation of Eqs. (2) and (3) gives

$$d\mu_O = d\mu_O^{\text{oxide}}, \quad (4a)$$

$$dp - dp' = d\left(\frac{2\gamma}{R}\right). \quad (4b)$$

The perturbation is also governed by Gibbs–Duhem equation [25],

$$s dT - \Omega dp - d\mu_O = 0, \quad (5a)$$

$$s' dT - \Omega' dp' - d\mu_O^{\text{oxide}} = 0, \quad (5b)$$

where Ω and Ω' are the molecular volumes of the gas and the oxide, respectively, and s and s' are the entropies per molecule of the gas and the oxide side, respectively. Solving Eqs. (4) and (5) for isothermal conditions yields

$$\frac{\Omega' - \Omega}{\Omega'} dp = d\left(\frac{2\gamma}{R}\right), \quad (6)$$

which upon neglecting Ω' with respect to Ω , using the gas law, $\Omega = k_B T/p$, and integration between p_0 and p gives

$$p = p_0 \exp\left(-\frac{2\gamma\Omega'}{Rk_B T}\right). \quad (7)$$

Eq. (7) gives the oxygen pressure that has to exist inside a void of radius R enclosed in an oxide in order for equilibrium to be attained throughout the heterogeneous oxide. This equation is known in classical thermodynamics as the Kelvin equation for equilibrium of a liquid (or a solid) with its vapor [25]. A plot of Eq. (7) is shown in Fig. 1 for UO_2 . The plot shows that the deviation from the reservoir oxygen partial pressure dictated by Eq. (7) is small for radii within the range of those observed for equilibrium voids in UO_2 [6].

In order to appreciate the result (7), i.e., the presence of oxygen gas in voids in any oxide, let us consider the following situations.

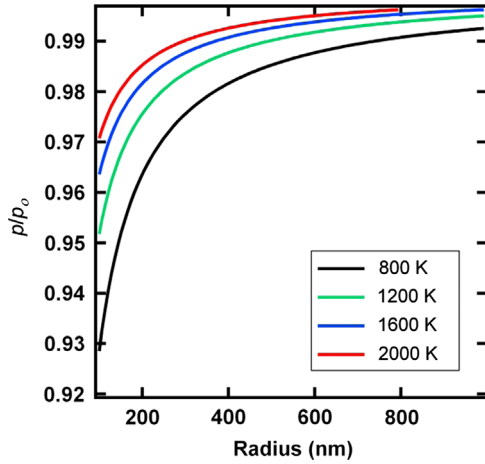


Fig. 1. Oxygen pressure inside a void within UO_{2+x} relative to that of the equilibrium reservoir as a function of void radius at 800, 1200, 1600 and 2000 K.

The first is the case of an infinite oxide in equilibrium with an oxygen reservoir at p_0 . In this case, the solid is assumed to be in a uniform equilibrium state. When a free surface is present, and aside from some perturbation of the defect state near the free surface, the semi-infinite solid in equilibrium with an oxygen environment is equivalent to an infinite solid in equilibrium with the same environment. If we now imagine a second situation in which a slab of the oxide with well separated surfaces is subject to oxygen pressure p_0 at one of its faces, this slab will not be under equilibrium unless the other face is also subjected to the same pressure p_0 . Any pressure difference will result in diffusion of atomic species across the slab. If we now imagine that one of the faces of this slab is curved, equilibrium will still require that on the side of the curved surface some oxygen pressure p must exist and its value must depend on the curvature of the surface and the remote pressure p_0 . In the limit of a small radius of curvature, the curved surface of the slab can be turned into a void in a semi-infinite solid. Increasing the separation of this void from the flat slab surface indefinitely now represents an isolated void in an infinite oxide having oxygen gas at pressure p . The implications of this finding are so important in the case of UO_2 because, being a gaseous species that is present in abundant quantities in this oxide material, oxygen should be expected to play an important role in the dynamics of voids nucleation and growth under irradiation. To the best of the authors' knowledge, there is no past evidence in the literature that oxygen has been considered important in void dynamics in UO_2 under irradiation.

2.2. Bulk thermodynamics

Having introduced the bulk state of the void, we now need to specify the chemical state of the bulk of the oxide. This can be achieved by using a point defect model that relates the defect and electronic carrier concentrations to the controlling parameters, i.e., temperature and oxygen partial pressure of the reservoir. We have introduced a point defect model [20] based on the formation energies calculated through density functional theory by Crocombette et al. [26]. The model is briefly quoted here for completeness.

The free energy change of the system due to disorder in the form of point defects and electronic carriers is given by

$$\Delta G = \sum_D \sum_q e_{D^q} n_{D^q} - T \Delta S_{\text{conf}} + n_e (E_c - e_F) + n_h (e_F - E_v) - T \Delta S_{\text{elect}}, \quad (8)$$

where e_{D^q} is the free energy of formation of a single atomic defect of type D and effective charge q , n_{D^q} is its count, ΔS_{conf} is the

configurational entropy due to introduction of atomic defects, n_e and n_h are the numbers of electrons and holes, respectively, e_F , E_c and E_v are the Fermi energy, conduction band minimum and valence band maximum, respectively, and ΔS_{elect} is the electronic carrier entropy [23]. Note that fractional concentrations, i.e. number per formula unit, are used throughout this paper. The entropies can be calculated as [27,28]

$$\Delta S_{\text{conf}} = k_B \ln W_{\text{conf}}, \quad (9a)$$

where

$$W_{\text{conf}} = \prod_D W_D = \prod_D \frac{N_D!}{\prod_{i=1}^r (n_{D^i}!) \cdot (N_D - \sum_{i=1}^r n_{D^i})!}, \quad (9b)$$

and

$$\Delta S_{\text{elect}} = k_B \ln W_e = k_B \ln \binom{N_c}{n_e} \cdot \binom{N_v}{n_h}, \quad (9c)$$

where in the above, N_D is the number of sites available for defect D and r is the number of its possible charge states. For electrons and holes, N_c and N_v are the number of states in the conduction and valence band, respectively. Using Eq. (9) into (8) and minimizing the free energy with respect to each species yields expressions for the fractional concentrations

$$c_{D^q} = n_D \frac{\exp[-(e_{D^q}/k_B T)]}{1 + \sum_q \exp[-(e_{D^q}/k_B T)]}, \quad (10)$$

where c_{D^q} is the fractional concentration of defects of type D and charge q and n_D is the number of available sites for D per formula unit of the oxide. For electrons and holes Eq. (10) can be used by replacing e_{D^q} with their counterparts as in Eq. (7) and considering them as two different types. The free energy of formation of defects can be written as

$$e_{D^q} = e_{D^q}^R + q e_F - T \Delta S_D - \mu_D(T, p_0), \quad (11)$$

where $e_{D^q}^R$ is the (internal) energy of formation, ΔS_D is the entropy of formation and μ_D is a reference chemical potential characteristic of the disorder state, cf. [20,26]. Given the temperature and oxygen partial pressure of the disorder state, the bulk composition can be calculated by adding the electroneutrality condition below and solving for the concentrations

$$\sum_D \sum_q q c_{D^q} + c_h - c_e = 0. \quad (12)$$

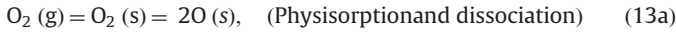
Once solved, the above model gives the point defect and electronic carrier concentrations in the bulk of an oxide at a given temperature T and immersed in an oxygen environment of a prescribed pressure p_0 . The results fix the boundary condition for the defect concentrations far in the bulk when solving for the spatial distribution of defects and electronic carriers densities around an isolated void.

2.3. Void-oxide interface

The solid oxide surface experiences the oxygen content of the void and that will lead to a chemical interaction. The interface necessitates the formation of surface excess in terms of adsorbed oxygen and subsurface modification to the composition. The adsorbed oxygen is chemisorbed and can acquire electrons from the oxide. Such electrons will reside in the *extrinsic* energy states introduced by the adsorbate. This is the ionosorption effect proposed by Hauffe [29–32]. When electrons are accommodated on the surface states, the near surface region builds up a positive charge and its composition is modified. The electrostatic potential difference obtained between the surface and the bulk effectively modifies the defect and electronic carrier concentrations. This

continues until a global electroneutrality is achieved at which the void has dictated the composition of its surrounding region.

The sequence representing interaction of the void oxygen with its surface can be modeled by the following scenario



The physisorption is described by Langmuir isotherm [30]. The dissociation is modeled by mass action

$$\frac{[\text{O}]^2}{[\text{O}_2]} = \exp\left(-\frac{\Delta G_c}{k_B T}\right), \quad (14)$$

where ΔG_c is the dissociation energy of the oxygen molecule on the surface of interest. The ionization reactions, Eqs. ((13b) and (13c)) can be modeled by Fermi statistics through the probability of occupying the extrinsic surface states; E_s , of O_2 and O by electrons [30,31]

$$\frac{[\text{O}_2^-]}{[\text{O}_2]} = \exp\left(-\frac{E_s(\text{O}_2) - e\phi}{k_B T}\right), \quad (15\text{a})$$

$$\frac{[\text{O}^-]}{[\text{O}]} = \exp\left(-\frac{E_s(\text{O}) - e\phi}{k_B T}\right). \quad (15\text{b})$$

Eqs. (15a) and (15b) represent a Maxwell–Boltzmann approximation to the Fermi–Dirac statistics. This approximation can easily be relaxed once information on the extrinsic surface states of UO_2 becomes available. The total surface charge can be found by combination of Eqs. (15a) and (15b) with the Langmuir isotherm to give

$$Q = e \left[\Gamma(T, p) \exp\left(\frac{e\phi - E_s(\text{O}_2) - e\Delta\phi}{k_B T}\right) + \sqrt{\Gamma(T, p)} \exp\left(\frac{e\phi - E_s(\text{O}) - e\Delta\phi - (1/2)\Delta G_c}{k_B T}\right) \right], \quad (16)$$

where Γ is the adsorbate coverage given by the Langmuir isotherm [20,30] and $\Delta\phi$ is the electrostatic potential difference between the surface and the oxide bulk. The solution of the local off-stoichiometry for the system must conform to the equality of surface and the total subsurface charge

$$Q = eN_U \int \sum_D \sum_q q c_{D^q} dV. \quad (17)$$

2.4. Local off-stoichiometry model

In order to resolve the spatial variation of the defect concentration in the vicinity of an isolated void, we solve a system of electrochemical diffusion equations in a static form. Starting from the electrochemical potential, η_{D^q} , representing the defects on the oxide lattice [21],

$$\eta_{D^q} = \mu_{D^q}^0 + RT \ln \frac{\gamma_D c_{D^q}}{1 - c_{D^q}} + qF\phi, \quad (18)$$

with ϕ being the electrostatic potential, F Faraday's constant, and γ_D the activity coefficient, the diffusive defect flux can be written in the form

$$J_D = -M_D \nabla \eta_{D^q}. \quad (19)$$

In the above, M_D is the mobility of defect D . Substituting Eq. (18) into Eq. (19) and then into the continuity equation yields

$$\frac{\partial c_{D^q}}{\partial t} = \theta_D \nabla^2 c_{D^q} + \frac{\theta_D q e}{k_B T} [c_{D^q}(1 - c_{D^q}) \nabla^2 \phi + (1 - 2c_{D^q}) \nabla c_{D^q} \cdot \nabla \phi], \quad (20)$$

where θ_D is the diffusivity of defect. Eq. (20) is a diffusion equation for defect D with effective charge q driven by the chemical and

electrostatic fields within the oxide. A similar expression for the diffusion of electronic carriers can be written

$$\frac{\partial c_{e,h}}{\partial t} = -\theta_{e,h} \nabla^2 c_{e,h} - \frac{\theta_{e,h} q_{e,h} e}{k_B T} [\nabla c_{e,h} \cdot \nabla \phi + c_{e,h} \nabla^2 \phi]. \quad (21)$$

The static form of Eqs. (20) and (21) can be obtained by setting the time derivative to zero which also cancels out the diffusivities θ . The electrostatic field is given by the solution of Poisson's equation,

$$\epsilon_r \epsilon_0 \nabla^2 \phi = -\sum \rho_D, \quad (22)$$

where ϵ_r is the relative dielectric constant, ϵ_0 is the dielectric permittivity of free space and $\rho_D = eN_U \sum q c_{D^q}$ is the local charge density due to all defect species.

With the appropriate electrochemical equilibrium boundary condition in the interior of the solid (far away from the void surface), the solution of the electrochemical diffusion problem above gives space-dependent concentration and electrostatic fields but constant electrochemical potential. In other words, there is not actually mass transport in the system associated with the solution of the steady state electrochemical diffusion problem stated above. Stated differently, the solution of this problem seeks to find the electro and chemical parts of a set of uniform electrochemical potentials of defects and electronic species as a function of distance from the void surface.

Eqs. (20)–(22) comprise a set of second order differential equations for the defects equivalent to a variational minimization of the free energy of the system. The only requirement for the solution is to fix the boundary conditions. These are provided on the bulk side by the point defect concentrations given through the point defect model, Section 2.2. The surface concentrations are given by

$$c_{D^q}^s = c_{D^q}^b \exp\left(\frac{q\Delta\phi}{k_B T}\right) \quad (23)$$

where $c_{D^q}^s$ is the surface concentration of defect D with charge q , $c_{D^q}^b$ is its bulk concentration given by the point defect model and, as stated previously, $\Delta\phi$ is the electrostatic potential difference between the bulk and the void surface. The overall charge electroneutrality condition; Eqs. (16) and (17), constrains the solution to the correct value of the $\Delta\phi$ where we assume a reference; $\phi(R) = 0$, at the void surface.

The spherical forms of Eqs. (17) and (20)–(22) are discretized using a central difference scheme which constitutes with Eq. (16) a nonlinear system of equations. The system is solved using Newton's Method and the Jacobian matrix is calculated and handled iteratively for an accurate solution. The system gives a form of the Jacobian that is sparse but non-symmetric with a full row resulting from Eq. (17). This exhausted the applicability of iterative methods and restricted us to direct solvers for which PARDISO routine (Parallel Sparse Direct and Multi-Recursive Iterative Linear Solvers) [33,34] is used to solve the Jacobian at each Newton's iteration.

2.5. Application to UO_{2+x}

In order to calculate the bulk defect concentrations, the point defect model requires the formation energies of each defect type. These were obtained from Crocombette et al. [26] for the set of defect types and charges admitted into this model, see Table 1. Admitted defect species are uranium vacancies, oxygen interstitials and vacancies. The thermodynamic state of UO_{2+x} is controlled by the temperature and oxygen partial pressure of the reservoir in equilibrium with the oxide. Therefore, the reference chemical potential in Eq. (11) are taken to be the equivalent of oxygen gas chemical potential at the temperature and oxygen

Table 1
Parameters used for the model applied to voids in UO_{2+x} .

Parameter	Symbol	Value	Units
Internal energy of formation [26] e_D^0 :	V_{U^0}	−3.75	eV
	O_i^-, O_i^+	0.0	eV
	O_i^*	−0.8	eV
	V_O^-	5.0	eV
	V_O^+	5.9	eV
	V_O^*	7.0	eV
Oxygen dissociation energy on (111) surface [40]	ΔG_c	1.66	eV/atom
Oxygen adsorbate surface state energy	$E_s(O)$	−0.5	eV
Dielectric constant of UO_2 [41]	ϵ_r	24	–
Electronic band gap of UO_2 [36]	$E_c - E_v$	2	eV
Density of electronic states of UO_2 [36]	N_c	1	State per molecular unit

pressure of interest. As such, reference chemical potential for uranium vacancies is $\mu_{V_U} = \mu_{O_2}(T, p_0)$, for oxygen vacancies is $\mu_{V_O} = -(1/2) \mu_{O_2}(T, p_0)$, and that for oxygen interstitials is $\mu_{O_i} = (1/2) \mu_{O_2}(T, p_0)$. The values were taken from [35]. For electronic carriers, the band gap and the density of states are obtained from [36].

The most important impact of the void surface comes through the surface state energy E_D^S in the dominant second term of Eq. (16). The energy state was inferred from the electronic density of states of UO_2 calculated by Yun et al. [37] using the Madelung model [31] and the idea of band center [38]. The value was estimated to be −0.5 eV (below the valence band maximum). The surface (111) was assumed in the model as it is the most stable of UO_2 [6,39]. The dissociation energy of an oxygen molecule over the (111) surface was calculated by Skomurski et al. [40]. Parameters input to the model for the case of voids in UO_{2+x} are contained in Table 1. The above parameter selection involves the approximation that, although the void is considered to be of a spherical shape, the properties of its surface are taken to be uniform and equivalent to those of a flat (111) surface. At elevated temperatures, the void surfaces may be atomically rough, which makes it possible to consider uniform surface properties. The use of (111) surface properties, however, is an approximation that must be checked as more data on the void surface morphology and defect states of UO_2 surfaces become available. In passing, it is important to point out that equilibrium voids in UO_2 may have non-spherical shapes as reported in [6].

3. Results and discussion

The view of a void within a disordered oxide as an oxygen gas inclusion whose pressure is controlled by the equilibrium state of the oxide brings more details to the interaction of such entities with the host oxide. A surface excess forming at the boundary results in the buildup of a surface charge that depletes negative charge from the surrounding oxide and modifies the potential landscape in the vicinity. The potential affects the chemistry of the oxide in the surrounding shell owing to the ionic nature of oxides as is accounted for in this model by the charge states of defects.

Defect concentration profiles are affected by the introduced electrostatic potential field. A negative surface charge in the form of ionosorbed O^- ions reduces the surrounding shell by increasing the oxygen vacancy concentration or, equivalently, depleting the uranium vacancy concentration. This is shown in Fig. 2 at select temperatures and oxygen pressure values which produce a bulk that is very close to exact stoichiometry. Fig. 2 shows the total defect concentration of each type regardless of its charge states. Orders of magnitude change in the defect concentrations in the

vicinity of voids can be seen, e.g., 3–4 orders of magnitude increase in the oxygen vacancy concentration is noted. Also, a change of larger magnitude is seen for the uranium vacancies. The controlling parameter that affects the magnitude of variation is the effective charge of the defect species. The dip in the uranium vacancy concentration is mainly due to the quadruply charged vacancy state which is found to be dominant in the bulk over all other charge states for the uranium vacancy at hyperstoichiometry. Therefore, the change in magnitude is enlarged by this fact as it is a translation of Eq. (23). On the other hand, oxygen vacancies are not dominant in most of the examples shown but are boosted towards the void surface due to their effective positive charge states, namely singly and doubly charged. The ramification of the found defect behavior is that the region near the interface of a gas inclusion in the oxide remains reduced, i.e., with a less oxygen content due to increasing the oxygen vacancy concentration and/or more metal content due to the decrease in the uranium vacancies. Further, from a microscopic point of view, the matrix-void reaction is not driven by the dominant defect species in the bulk, rather by the one that dominates the interface, i.e., oxygen vacancies as this study shows in the case of UO_{2+x} . The interaction magnitude depends on the availability of such defect types at the interface or the concentration of the significant species at the interface. Such concentration variation is a function of the bulk state; determined by the temperature and oxygen partial pressure, and the void radius as discussed below by the global measure of the model solutions.

The variation of defect concentration translates into change in the disorder state of the oxide. This is manifested by the off-stoichiometry variation in the zone around the void. Fig. 3 shows, on a logarithmic scale, the off-stoichiometry variation around a void of 100 nm radius at 1400 and 1700 K and several equilibrium oxygen partial pressure values as a function of radial distance. The chosen oxygen partial pressure values represent a wide range of off-stoichiometric bulk states. A solid line represents a hyperstoichiometric state of UO_{2+x} while a dashed line represents a hypo-stoichiometric case; therefore, the sharp dips correspond to an exactly stoichiometric point of the oxide. The variation occurs throughout a shell thickness between a few nanometers to several tens of nanometers around the void, depending on the remote oxygen pressure and temperature. Off-stoichiometry laid in this manner is a mesoscale variable that carries important implications about the heterogeneity of the defect state of an oxide. As a consequence of the seen off-stoichiometry variation, an array of voids within a UO_{2+x} matrix would imply an overall off-stoichiometric state that is different from the ideal value for a void-free case. It is therefore safe to say that the equilibrium state of a disordered oxide, in this case UO_{2+x} , is a function not only of the thermodynamic variables; temperature and oxygen

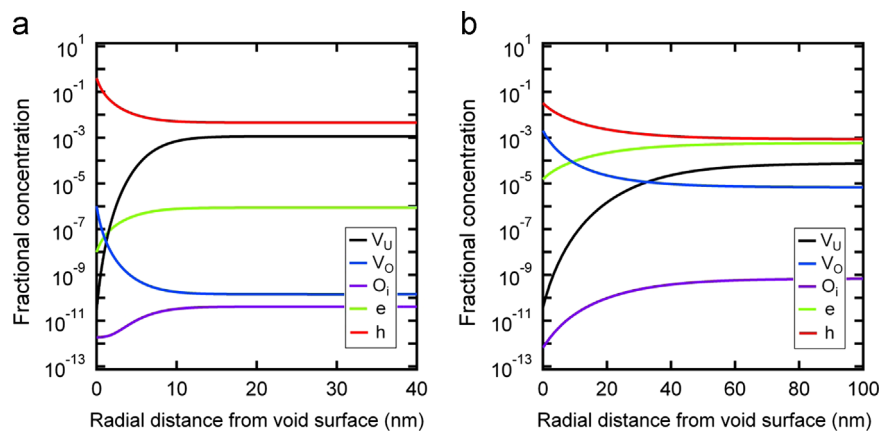


Fig. 2. Defect concentrations as a function of radial distance from the surface of a void of a 100 nm radius at (a) 1200 K and (b) 1600 K, with $p_{\text{O}} = 10^{-19}$ atm for both.

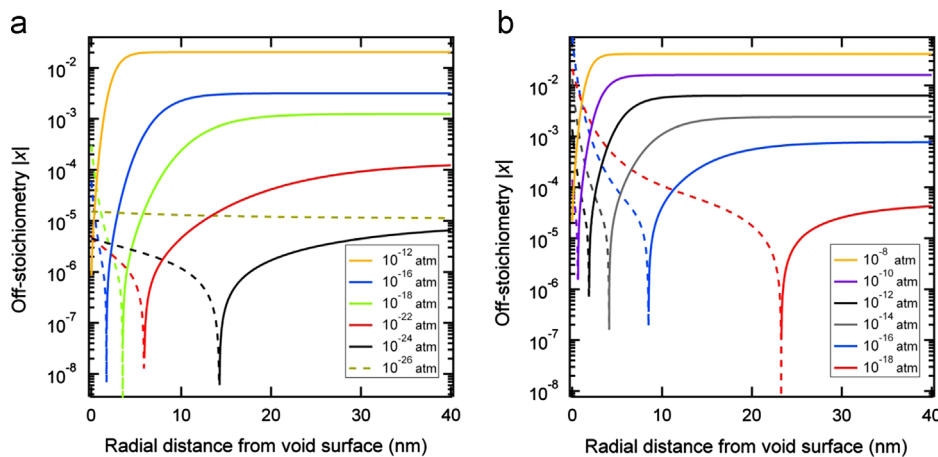


Fig. 3. Off-stoichiometry variation through the shell surrounding a 100 nm radius void in UO_{2+x} at two temperatures. (a) 1400 K and (b) 1700 K, and several bulk states; represented by the remote oxygen partial pressure. Note: solid lines represent positive off-stoichiometry values, i.e., hyper-stoichiometry, and dashed lines represent negative off-stoichiometry values, i.e., hypo-stoichiometry.

partial pressure but also, and equally important, a function of its microstructure details through the created mesoscale fields. Such microstructure is itself a function of the history of the oxide system under consideration. Disordered oxides, i.e., oxides which are able to exist in off-stoichiometric states, exhibit strong variations in their physical properties over small off-stoichiometry increments, especially around exact stoichiometry where the defect chemistry varies significantly. The obtained variations in off-stoichiometry significantly influence the physical properties of the oxide in such a way that corresponds to the conclusion mentioned above about the determination of the oxide's state. This necessitates the consideration of mesoscale details when characterizing such oxides.

The defect state of the void-free bulk is related mainly to the temperature and equilibrium oxygen pressure and is presented in terms of uniform defect concentrations. The behavior of the void-oxide system, however, can be studied in terms of quantities such as the electrostatic potential difference across the space charge region (influence shell) and the thickness of this region. The electrostatic potential difference across the influence shell is depicted in Fig. 4(a), where the calculated potential difference is plotted as a function of the oxide off-stoichiometric state, shown here in terms of the remote oxygen pressure, for a void of 100 nm at several temperatures. The potential difference value peaks at exact stoichiometry or very close to it and diminishes symmetrically towards either hypo- or hyper-stoichiometry. This measure is related to the magnitude of variation in the defect concentrations. More importantly, the electrostatic potential difference represents

an additional kinetic barrier across the void surface-shell region for defects to overcome under non-equilibrium conditions giving rise to diffusion in the direction of the surface or defect absorption or emission from the surface itself, e.g., under irradiation. Any evolution of the void should be controlled by this barrier whether caused by a change in the oxide bulk composition or a temperature change or introducing excess defects through irradiation. Predictions of the current model for the electrostatic barrier around voids tie it to the thermodynamic state of the oxide and indicate that the void interaction with the oxide is a strong function in such conditions. In other words, the microstructure response of the oxide in the presence of voids will differ depending on its initial state. This response is also a function of the mesoscale details calculated by the model in the form of defect concentrations which mediate the evolution. The situation can also be complicated when an array of voids coexist at small separations in the oxide. In such case, the evolution of the whole ensemble of voids is checked by the magnitude of their barriers which are not necessarily of equal magnitude. Influence shell thickness is another measure of the system behavior.

Fig. 4(b) shows the thickness over which defects concentrations vary near the void surface, as a function of the oxide state given by the remote oxygen pressure, for several temperatures. The shell thickness is mostly a monotonic function of the off-stoichiometry that increases as the oxide goes from hyper-stoichiometry to hypo-stoichiometry. The leveling off of the thickness at very low oxygen partial pressures, corresponding to a strongly hypo-stoichiometric

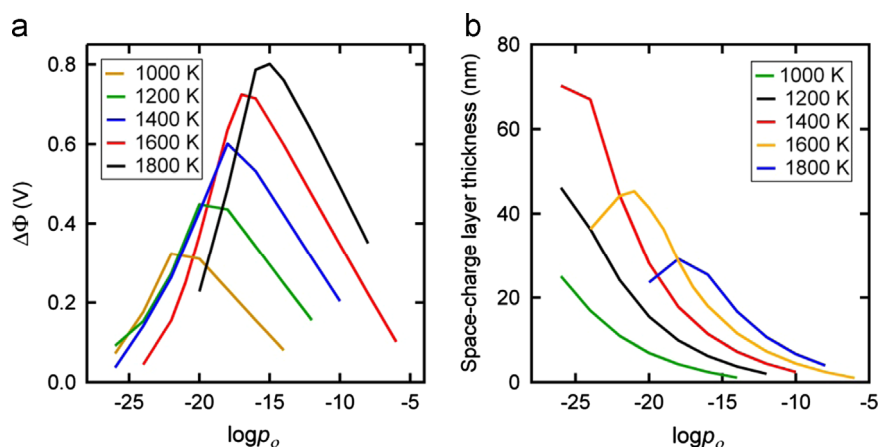


Fig. 4. Global measures of the void electrochemical effect in terms of the electrostatic potential difference across the influence shell, (a), and thickness of the influence shell, (b), for a wide range of temperature and bulk off-stoichiometry in the case of a void with a 100 nm radius.

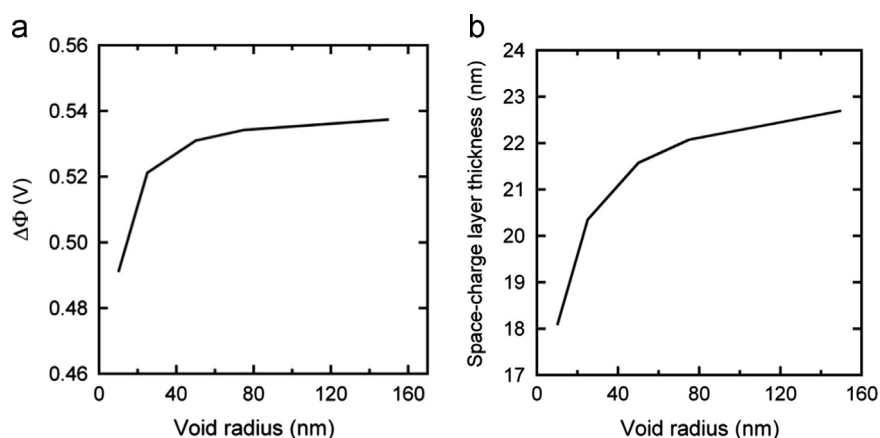


Fig. 5. The radius effect on two measures of the solutions: (a) the electrostatic potential difference across the space-charge, and (b) the space-charge shell thickness around the void at 1400 K and oxygen partial pressure of 10^{-19} atm.

UO_{2+x} , represents a diminishing extent of oxygen ionosorption giving almost constant defect concentrations. Thus, the bulk composition extends to the interface only at a limiting case where the electrochemical effect of the void is diminished. It is worthwhile to note that obtaining unique values for such measures is possible only through the solution of the differential equations; Eqs. (20)–(22) in conjunction with the global electroneutrality condition, Eqs. (16) and (17). Introduction of the ionosorption theory into this model have filled a gap that can only be filled through more physics based details.

The effect of void radius on the previous global parameters is shown in Fig. 5. The parameters correlated to the void radius are the electrostatic barrier and the space-charge thickness for the case of 1400 K and equilibrium oxygen pressure of 10^{-19} atm over a range of radii between 10 nm and 160 nm. It can be seen that the variation in these parameters almost saturates beyond a radius of 50 nm where it approaches a value that corresponds to the flat surface limit [20]. The radius or curvature effect comes into play through Kelvin equation; Eq. (7), which in turn affects Eq. (16) through the coverage Γ , and the spherical form of Eqs. (17) and (20)–(22). Though this shows consistency with flat surface results, the variation is minute rendering the curvature effect on the model results insignificant. It is to be noted here that the void size comes to play once in the form of the curvature, which defines the physical and chemical boundary condition at the surface, and another time as a parameter that defines the geometry of the solution of the electrochemical diffusion and electrostatic problems.

We have used the void surface curvature to ensure the thermodynamic consistency of a void within a disordered oxide in equilibrium with a thermochemical reservoir of oxygen. It is safe to say, then, that a void with an oxygen pressure abiding by Eq. (7) is in thermodynamic equilibrium with that reservoir. However, with vacuum-like orders of magnitude of equilibrium oxygen partial pressure that are known for UO_{2+x} , the void will have a pressure of a lesser value according to Eq. (7). Using macroscopic equation of state, the number of molecules to be found within a small void of ~ 10 –100 nm radius is actually a fraction. We, therefore, see the void with this thermodynamic state in a time average sense, i.e., gas matter is accommodated in the void such that the gas pressure on average is given by Eq. (7). Moreover, in deriving Eq. (7), we used the ideal gas law as the equation of state for the gas inside the void. This is sound given the void sizes addressed and the very low pressure values. A void with a size of tens of nanometers is well represented by Kelvin equation in the form of Eq. (7) [42]. One can conceive the idea of this model for the electrochemical effect of a void within an oxide from the oxide side. The oxide, as a mediator for the void-reservoir equilibrium, perceives the void with that value of oxygen pressure regardless of the actual void content. The intermediate surface excess, i.e. the adsorbate, does not necessarily relate to the oxygen content of the void; rather between two such entities; i.e., the oxide and the void, such an extent of adsorption has to exist at thermodynamic equilibrium. In other words, thermodynamic equilibrium of the surface does not care about the kinetic pathways which had lead up to its attainment or whether the surface

oxygen originates in the oxide matrix or in the void. Further studies are required in regard to the state of oxygen both on the surface and inside of small voids, including quantum and chemical descriptions of the oxygen atoms and/or molecules.

It is also important to note that voids undergo faceting at low temperatures. At high temperatures, the surface of voids may be atomically rough and have nearly spherical shapes, a view that we have adopted in the current model. Castell [6] noted this fact and explained that by lowering the temperature towards the room temperature, voids show faceting according to the energy minimization of the surface energy and that the kinetics of this process depends on the void size and the rate of cooling where some voids would have no time to adopt to shapes that conform to thermodynamic equilibrium at the low temperature. Here, we have chosen the most stable surface termination for UO_2 and assumed a spherical shape for two reasons. First, the temperature range used to solve the model is of an intermediate range where the phenomenon of faceting is less significant. And second, it is a good approximation as the surface energy comes into consideration through Kelvin equation which does not drastically affect the results.

The current model can be validated experimentally using a number of techniques. One technique may take advantage of the fact that the electrical conductivity of defective oxides is sensitive to charged defect concentrations. Void may affect the conductivity of an ionic oxide both geometrically by the presence of a void space chemically by altering the charged defect concentration near their surfaces. Techniques similar to those applied to the grain boundary effect on conductivity in semiconductor oxides [23,43] may therefore be applied. In such techniques, the conductivity is measured as a function of grain size and thermodynamic state, i.e., temperature, oxygen partial pressure and dopant concentrations. In the case of voids, the analogous approach is to examine the conductivity variations for the oxide with void density and sizes at various thermodynamic states. This suggested approach can thus measure the effect of the void structure indirectly [44].

4. Conclusions

A model that brings into consideration the electrochemical effect of voids in oxides is presented. An important finding of this model is that, a void within an oxide, in this case UO_{2+x} , should necessarily contain oxygen based on thermodynamic arguments. Such oxygen content gives rise to interaction with its surface which is modeled using the ionosorption theory. Further, an electrochemical model to calculate the modification in defect composition as a result is devised and solved for several thermodynamic states of UO_{2+x} . Parameters from published electronic structure calculations were tied to the thermodynamic state and incorporated into the model. The model predicts that a void within an oxide must affect the composition of this oxide within a shell of influence by controlling the defect concentrations in this shell. The size of such shells of influence is found to be comparable to or larger than the void size. The model results include the electrostatic potential barrier that controls the void interaction, via defects and electronic carriers, with the oxide and its mesoscale elements. As such, calculation of the value of the electrostatic barrier is essential to understanding of voids evolution in an oxide. The electrostatic barrier corresponding to such variations is of a considerable magnitude and varies strongly with the off-stoichiometric state with which the void coexists. While we have applied our model to the case of UO_{2+x} as a typical disordered oxide at various temperatures and off-stoichiometric states and calculated the atomic defects and electronic carrier profiles around an equilibrium void, the model applies in principle to any

disordered solid ionic oxide. An extension of this model to complex structures of voids and/or other mesoscale elements within an oxide will help us resolve the mesoscale defect density variations as well as the response of the microstructure to variations in environment conditions and irradiation when kinetics are considered.

Acknowledgment

This material is based upon work supported as part of the Center for Materials Science of Nuclear Fuel, an Energy Frontier Research Center funded by the U.S. Department of Energy, Office of Science, Office of Basic Energy Sciences under award number FWP 1356 through subcontract number 00122223 at Purdue University.

References

- [1] G. Was, *Fundamentals of Radiation Materials Science*, Springer-Verlag, Berlin, Heidelberg, Germany, 2007.
- [2] D. Olander, *Fundamental Aspects of Nuclear Reactor Fuel Elements*, U.S. Energy Research and Development Administration, Office of Public Affairs, Technical Information Center, 1976.
- [3] K. Nogita, K. Une, *J. Nucl. Sci. Technol.* 30 (1993) 900.
- [4] J. Spino, K. Vennix, M. Coquerelle, *J. Nucl. Mater.* 231 (1996) 179.
- [5] K. Maeda, K. Katsuyama, Y. Ikusawa, S. Maeda, *J. Nucl. Mater.* 416 (2011) 158.
- [6] M. Castell, *Phys. Rev. B* 68 (2003) 1.
- [7] R. Huang, K.R. Hebert, L.S. Chumbley, *J. Electrochem. Soc.* 151 (2004) B379.
- [8] A. Bacciochini, J. Ilavsky, G. Montavon, A. Denoirjean, F. Ben-ettouil, S. Valette, P. Fauchais, K. Wittmann-teneze, *Mater. Sci. Eng. A* 528 (2010) 91.
- [9] F. Lai, M. Li, H. Wang, H. Hu, X. Wang, J.G. Hou, Y. Song, Y. Jiang, *Thin Solid Films* 488 (2005) 314.
- [10] G. Martin, P. Garcia, C. Sabathier, L. Van Brutzel, B. Dorado, F. Garrido, S. Maillard, *Phys. Lett. A* 374 (2010) 3038.
- [11] D.S. Aidhy, P.C. Millett, D. Wolf, S.R. Phillpot, H. Huang, *Scr. Mater.* 60 (2009) 691.
- [12] D.S. Aidhy, D. Wolf, A. El-Azab, *Scr. Mater.* 65 (2011) 867.
- [13] R. Bullough, J.R. Willis, *J. Nucl. Energy.* 32 (1969) 76.
- [14] D.C. Ahn, P. Sofronis, R. Minich, *J. Mech. Phys. Solids* 54 (2006) 735.
- [15] A.M. Kosevich, I.G. Margvelashvili, Z.K. Saralidze, *Sov. Phys. Solid State* 7 (1965) 370.
- [16] A. Seeger, U. Gosele, *Phys. Lett.* 61A (1977) 423.
- [17] A.I. Ryazanov, C. Kinoshita, *Nucl. Instrum. Methods Phys. Res. B* 191 (2002) 65.
- [18] J. Nowotny, *Mater. Sci. Forum* 29 (1988) 99.
- [19] M.A. Blesa, A.E. Regazzoni, J.G. Maroto, *Mater. Sci. Forum* 29 (1988) 31.
- [20] A.-R. Hassan, A. El-Azab, C. Yablinsky, T. Allen, *J. Solid State Chem.* 204 (2013) 136.
- [21] N. Swaminathan, J. Qu, Y. Sun, *Philos. Mag.* 87 (2007) 1705.
- [22] K.L. Kliewer, J.S. Koehler, *Phys. Rev.* 140 (1965) A1226.
- [23] J. Maier, *Physical Chemistry of Ionic Materials, Ions and Electrons in Solids*, Wiley & Sons, Ltd., Chichester, UK, 2004.
- [24] A. Tschope, *Solid State Ion.* 139 (2001) 267.
- [25] R. Defay, I. Prigogine, A. Bellemans, D.H. Everett, *Surface Tension and Adsorption*, Longmans, Green & Co Ltd., Bristol, 1966.
- [26] J.-P. Crocombette, D. Torumba, A. Chartier, *Phys. Rev. B* 83 (2011) 1.
- [27] N.W. Ashcroft, N.D. Mermin, *Solid State Physics*, Holt Saunders, Philadelphia, 1976.
- [28] S. Kasamatsu, T. Tada, S. Watanabe, *Solid State Ion.* 183 (2011) 20.
- [29] K. Hauffe, *Adv. Catal.* VII (1955) 213.
- [30] S.R. Morrison, *The Chemical Physics of Surfaces*, Plenum Press, New York, 1977.
- [31] C.O. Park, S.A. Akbar, *J. Mater. Sci.* 38 (2003) 4611.
- [32] A. Flood, *The Solid Gas Interface*, Marcel Dekker, New York, 1967.
- [33] O. Schenk, K. Gärtner, *Electron. Trans. Numer. Anal.* 23 (2006) 158.
- [34] O. Schenk, A. Wächter, M. Hagemann, *Comput. Optim. Appl.* 36 (2007) 321.
- [35] I. Barin, *Thermochemical Data of Pure Substances*, VCH, Weinheim, Federal Republic of Germany, 1989.
- [36] P. Ruello, G. Petot-Ervas, C. Petot, L. Desgranges, *J. Am. Ceram. Soc.* 88 (2005) 604.
- [37] Y. Yun, H. Kim, H. Lim, K. Park, *J. Korean Phys. Soc.* 50 (2007) 1285.
- [38] Y.-L. Lee, J. Kleis, J. Rossmeisl, Y. Shao-Horn, D. Morgan, *Energy Environ. Sci.* 4 (2011) 3966.
- [39] H. Idriss, *Surf. Sci. Rep.* 65 (2010) 67.
- [40] F. Skomurski, L. Shuller, R. Ewing, U. Becker, *J. Nucl. Mater.* 375 (2008) 290.
- [41] N. Hampton, G.A. Saunders, J.H. Harding, A.M. Stoneham, *J. Nucl. Mater.* 149 (1987) 18.
- [42] A. Saito, H.C. Foley, *AIChE J.* 37 (1991) 429.
- [43] A. Tschope, E. Sommer, R. Birringer, *Solid State Ion.* 139 (2001) 255.
- [44] R.A. De Souza, *Phys. Chem. Chem. Phys.* 11 (2009) 9939.